Reconstructing the ocean's mesopelagic zone carbon budget: sensitivity and estimation of parameters associated with prokaryotic remineralization

Chloé Baumas[1]*#, Robin Fuchs[1,2]*, Marc Garel[1], Jean-Christophe Poggiale[1], Laurent Memery[3], Frédéric A.C. Le Moigne[1,3]#, Christian Tamburini[1]

Both authors contributed equally

[1]Aix Marseille Univ, Université de Toulon, CNRS, IRD, MIO UM 110, Marseille, France

[2]Aix Marseille Univ, CNRS, I2M, Marseille, France

[3] LEMAR Laboratoire des Sciences de l'Environnement Marin, UMR6539, CNRS, UBO, IFREMER, IRD, Plouzané, Technopôle Brest-Iroise, France

#Corresponding author : cbaumas@stanford.edu

Abstract

Through the constant rain of sinking marine particles in the ocean, carbon (C) trapped within is exported into the water column and sequestered when reaching depths below the mesopelagic zone. Atmospheric CO_2 levels are thereby strongly related to the magnitude of carbon export fluxes in the mesopelagic zone. Sinking particles represent the main source of carbon and energy for mesopelagic organisms, attenuating the C export flux along the water column. Attempts to quantify the amount of C exported versus consumed by heterotrophic organisms have increased in recent decades. Yet, most of the conducted estimations have led to estimated C demands several times higher than the measured C export fluxes. The choice of parameters such as growth efficiencies or various conversion factors is known to greatly impact the resulting C budget. In parallel, field or experimental data are sorely lacking to obtain accurate values of these crucial overlooked parameters. In this study, we identify the most influential of these parameters and perform inversion of a mechanistic model. Further, we determine the optimal parameter values as the ones that best explain the observed prokaryotic respiration, prokaryotic production, and zooplankton respiration. The consistency of the resulting C-budget suggests that such budgets can be adequately balanced when using appropriate parameters.

Keywords: Biological carbon pump, Optimization methods, Carbon budget, Mesopelagic zone, prokaryotic carbon demand, model inversion

1. Introduction

The biological carbon pump (BCP) is the main mechanism by which CO_2 is exported and stored in the deep ocean in the long term. This ecosystem service is defined as the sum of the biological processes that lead to carbon export from the euphotic zone into the deep ocean (Eppley and Peterson 1979). This process exports from 5 to 20 Gt C yr^{-1} in the form of particulate organic carbon (POC) gravitationally sinking from the sunlit ocean to the mesopelagic zone typically located between 200 and 1000 m (Henson et al. 2011). Therefore, atmospheric CO_2 levels are strongly related to any change in carbon export into the mesopelagic zone (Kwon et al. 2009). Five downward pathways of organic matter export to the mesopelagic zone are defined: phytoplankton (senescent cells, colonies, spores, cysts), zooplankton (carcasses or fecal pellets), aggregates (marine snow of different compositions including the two latter categories), vertical migration of zooplankton and mixing/diffusion/advection (Siegel et al. 2016; Le Moigne 2019).

Gravitational sinking POC supply, combining the 3 first pathways described above, constitutes the main organic carbon input to the mesopelagic zone (Boyd et al. 2019). Consequently, the downward flux of organic carbon is attenuated with increasing depth as it is fragmented, metabolized and remineralized by different biological processes until only the refractory material remains. The majority of POC flux attenuation occurs in the mesopelagic zone (Martin et al. 1987; Marsay et al. 2015; Fuchs et al. 2022). The remineralization of exported carbon is mainly performed by two types of organisms: microorganisms (mostly heterotrophic prokaryotes i.e. Bacteria and Archaea) and zooplankton. Heterotrophic prokaryotes primarily use dissolved organic carbon (DOC) as a source of carbon. However, some prokaryotes, colonizing particles upon formation, undergo changes in environmental conditions during their descent, such as the increase of the hydrostatic pressure and the variations of temperature (Tamburini et al. 2003, 2021; Baumas et al. 2021). Such particle-attached prokaryotes primarily use POC as a carbon source. Only organic matter of size below 600 Da diffuses directly through prokaryotic membranes, therefore attached prokaryotes produce ectoenzymes required to solubilize larger molecules (Weiss et al. 1991). Smith et al. (1992) observed that the amount of DOC produced by ectoenzymatic solubilization of POC may be 10 to 100 times greater than the absorption capacity of a cell. DOC is thereby released into the surrounding

water (the so-called solubilization). This increases the amount of DOC available for free-living prokaryotes. In addition, several types of zooplankton are involved in marine particles: POC-feeding detritivores (e.g. copepods), prokaryotes consumers (e.g. flagellates), and carnivores (e.g. chaetognaths). Besides, zooplankton lose POC through excretion (moult, mucilage, urine), fecal pellets (decomposed organic matter), and sloppy feeding. Giering et al. (2014) specify that 30% of a particle supplied by the downward flux is fragmented by the action of the detritivores and is transformed into suspended matter.

Given their importance regarding the BCP, all the processes described above were extensively studied in the last decades (e.g. Alldredge and Silver 1988; Smith et al. 1992; Kiørboe et al. 2002, 2003; Kiørboe 2003; Lampitt et al. 2008; Steinberg et al. 2008; Iversen et al. 2010; Giering et al. 2014; Koski et al. 2020 and references therein). However, the scientific community has struggled to reconcile the mesopelagic carbon budget with measurements and estimates showing a biological carbon demand often greater than the amount of known organic carbon sources (Reinthaler et al. 2006; Steinberg et al. 2008; Burd et al. 2010; Collins et al. 2015; Boyd et al. 2019). In other words, the measured export flux cannot sustain measured metabolic demands of prokaryotes and zooplankton altogether in the mesopelagic zone, leading to a discrepancy in C budgets.

A first explanation may lie in the choices of the boundaries of the mesopelagic zone used to integrate fluxes and to estimate the carbon budget as investigated in Fuchs et al. (2022). Indeed they specifically designed a method to determine from CTD-cast variables (fluorescence, O2 concentration, potential temperature, salinity, and density) accurate boundaries which vary in space and time. With their method named RUBALIZ, they show that 90% of the POC flux attenuation occurs within new determined boundaries which is not the case of the fixed 200-1000m often used. Besides, integrating prokaryotic C demand within RUBALIZ boundaries helps to reduce the discrepancy. Other sources of discrepancy may be found focusing on the carbon demand of prokaryotes (which are responsible for the final step of the remineralization), whose estimation is usually provided by adding rates of prokaryotic heterotrophic production (PHP) to that of prokaryotic respiration (PR) (Burd et al. 2010). PHP rates are often measured from tritiated leucine incorporation rates in incubations which are then multiplied by a conversion factor Leu/Carbon (CF) (Kirchman et al. 1985). The PR is more challenging to measure (especially in the dark ocean, (Nagata et al. 2010) and, therefore, often estimated from measurements of PHP and a prokaryotic growth efficiency (PGE) taken from the literature (as PR = PHP x (1-PGE)/PGE, del Giorgio and Cole 1998). Unfortunately, *in-situ* measurements

99 of both CF and PGE are time-consuming and operationally complex to perform (especially for

100 the mesopelagic zone). In addition, such data for particle-attached prokaryotic communities are

101 scarce since the adequate sampling devices (to specifically sample biologically intact sinking

102 particles) were only recently validated (Baumas et al. 2021). Besides, PHP and PR data are

103 usually obtained after decompression or carried out from experiments at atmospheric pressure,

104 being a source of misevaluation (Tamburini et al. 2013). As a result, mean values from global

105 literature compilation or theoretical values are often used as references for both CF or PGE

106 (Burd et al. 2010; Giering and Evans 2022) and may be far from the actual *in situ* values.

107 In parallel, model predictions help to estimate unmeasurable processes along with the

108 comparison and validation of data. The biological processes occurring in the mesopelagic zone

109 are not yet well constrained (see sections above). Consequently, only a few models specifically

110 designed to assess the fluxes governing the BCP in the mesopelagic zone exist (e.g. Tian et al.

111 2000; Anderson and Ryabchenko 2009; Anderson and Tang 2010; Fennel et al. 2022). For

112 instance, the model developed by Anderson and Tang (2010) enables the evaluation of the

113 remineralization of different compartments such as particle-attached prokaryotes to sinking and

114 suspended particles, free-living prokaryotes and up to six trophic levels of zooplankton. This

115 model describes the various known biological processes involved in the BCP system. However,

116 the model also requires to be set up with parameters such as the PGE. For example, Anderson's

117 model requires 20 parameters which often present large uncertainties.

118 Giering et al. (2014) attempted to reconcile carbon input and biological carbon demand in the

119 mesopelagic zone using the Anderson and Tang (2010) model and measurements carried out

120 in the North Atlantic (Porcupine Abyssal Plain site, 49.0°N 16.5°W, summer 2009). They

121 found that prokaryotes were responsible for 70-92% of the remineralization of organic carbon.

122 In this study, the model results were consistent with the measurements performed *in situ*,

123 showing a reconciliation of the carbon budget between 50 and 1000 m depths. Giering et al.

124 (2014) balanced their C-budget by using a rather low CF (CF = 0.44 kg C mol^{-1}) compared to

125 the one generally used in the literature (CF = 1.55 kg C mol^{-1}) and a PGE of 8% for free-living

126 prokaryotes and 24% for particle-attached prokaryotes. All these values were chosen as

127 medians of literature values compiled from various measurement methods. Wisely choosing

128 these parameter is therefore crucial to determine the reconciliation or the imbalance of carbon

129 budget.

130 In this respect, we rely on model inversion methods (Tarantola 2005) to provide meaningful

131 estimations of parameters of interest. For a given phenomenon, inversion methods rely on a

132   model taking as input the parameters to be estimated and whose outputs can be compared with

133   *in situ* measurements. The inversion procedure thus gives the value of the parameters that best

134   replicate the *in situ* measurements. This type of procedure has already been used in

135   oceanography modeling. For instance, Saint-Béat et al. (2018) studied phytoplankton marine

136   food web in the Arctic and Saint-Béat et al. (2020) examined pelagic ecosystems of two

137   different zones in the Arctic Baffin Bay using inversion method and sensitivity analyses to

138   identify which biological processes impact the most the planktonic ecosystem functioning.

139   Here, we investigate the impact of widely but inadequately used parameters associated with

140   the prokaryotic remineralization (e.g. CF, PGEs) on the magnitude of the discrepancy. Our

141   aims are: 1) to highlight the most sensitive parameters for which the determination of an

142   accurate value is critical in the context of balancing the mesopelagic carbon budget; 2) to

143   perform a mathematical inversion method to estimate the most plausible *in situ* values of the

144   most sensitive parameters from a limited field dataset; 3) to discuss our results in the context

145   of mesopelagic carbon budget.

146 2. Material & methods

147 2.1 *In situ* Data

148   Most of the data used in this study originated from the DY032 (June-July 2015) cruise at the

149   PAP (Porcupine Abyssal Plain) site in the North Atlantic onboard the RRS Discovery. Some

150   data unavailable for DY032 were estimated from a previous PAP cruise, D341 (July-August

151   2009). Most of the *in situ* data were compiled from already published cruise data (e.g. Giering

152   et al. 2014; Belcher et al. 2016; Baumas et al. 2021; Fuchs et al. 2022). Their post-treatments

153   to suit our study framework are described below. Additionally, we used data (ectoenzymatic

154   activities along with total hydrolysable amino acids and carbohydrates, depth profile of

155   heterotrophic prokaryotic production and respiration under *in situ* pressure versus atmospheric)

156   from the PEACETIME cruise (Guieu et al. 2020) that occurred in May 2017 in the

157   Mediterranean Sea to illustrate some points in our discussions (see supp data).

158 2.1.1 Carbon fluxes

159 a) Determination of the Active Mesopelagic zone boundaries

160   Fuchs et al. (2022) introduced the "RUBALIZ" method, using CTD data, which allows the

161   estimation of vertical boundaries targeting the zone of the dark ocean where most of the POC

fluxes attenuation occurs. At station PAP during cruise DY032, this so-called "Active Mesopelagic Zone" was located between 127 and 751 m.

b) Carbon inputs

The POC inputs to the active mesopelagic zone mainly involve the gravitational export of POC. Gravitational input was taken from Fuchs et al. (2022) who fitted a power law Martin curve (b of 0.84) on data obtained from 30 to 500m using Marine Snow Catcher (Belcher et al. 2016). However, gravitational input is not the only POC input known in the literature. Recently, Boyd et al. (2019), provided an estimation of other particle-injection pumps (PIPs) such as the mixed layer pump, physical pump, the seasonal lipid pump or the active transport related to metazoans migrations. At the PAP site during summer, only the eddy subduction pump, metazoans migrations, and large-scale physical pumps were relevant to take into account. Other PIPs do not correspond to the location and season considered in our study. From Boyd et al. (2019) review, these three particle-injection pumps seem to represent altogether around 52% of the gravitational export of POC. We therefore add up this proportion of POC to the purely gravitational inputs. This yields an overall POC flux of 134 mg C m^{-2} d^{-1} exported into the active mesopelagic zone. The corresponding net POC input is 117 mg C m^{-2} d^{-1} (that is POC fluxes at the end - 751 m - of the active mesopelagic zone subtracted to the one at the start - 127 m - for PAP DY032).

DOC inputs are taken from Giering et al. (2014) and are considered as the sum of direct DOC export via physical processes (advection-diffusion) and active flux from zooplankton migrations. We estimated from their extended Data Fig. 2 that the DOC gradient below 100m is hardly visible meaning that physical vertical DOC export is insignificant for the active mesopelagic zone which is studied here. As a result, we set the DOC export at 3 mg C m^{-2} d^{-1}, which corresponds only to the active flux from zooplankton migrations from Giering et al. (2014).

c) Carbon demands

As explained above, prokaryotic carbon demand is generally assessed by adding rates of prokaryotic heterotrophic production (PHP) to that of prokaryotic respiration (PR). PHP of non-sinking prokaryotes (that is, free-living and attached to suspended particles prokaryotes) are derived from leucine incorporation measurements on seawater samples and are taken from Fuchs et al. (2022). These data did not permit the separation of the free-living from attached to suspended particles (Baumas et al. 2021). Hence, in the sequel, we no longer make this

distinction and group both types under the term "non-sinking prokaryotes". During DY032, Marine Snow Catchers (MSC) were deployed to separate slow and fast-sinking particles from 100L of samples (Riley et al. 2012; Baumas et al. 2021). PHP rates associated with prokaryotic communities of fast-sinking particles were taken from Baumas et al. (2021) and slow-sinking particles are presented here. Briefly, slow-sinking particle fractions were sampled in the 7L base of the MSC. Samples were incubated and leucine incorporation rates were measured as for fast-sinking particles in Baumas et al. (2021). The formula described in Baumas et al. (2021) was then applied to normalize to 100L as particles were concentrated in 7L after 2h of decantation and to remove the contribution of non-sinking prokaryotes which were initially in this compartment around slow-sinking particles of interest. Total sinking prokaryotes PHP rates were obtained by adding both fast-sinking and slow-sinking prokaryotes PHP rates. In addition, we were able to use the respiration rates of fast-sinking particle-attached prokaryotes particles obtained at the PAP site during the DY032 cruise by Belcher et al. (2016). For each depth (30-500m) the mean total O_2 consumption per particle in nmol particle^{-1}d^{-1} was converted to mg C m^{-3} d^{-1} (assuming a respiration quotient $RQ(CO_2/O_2) = 1$) by multiplying by the total number of particles (i.e. fecal pellets + phytoplanktonic aggregates) and dividing by 95L which is the volume of the MSC used (Riley et al. 2012). It is also important to note that PR for slow-sinking particles is missing. Thus, when we mention the respiration of sinking prokaryotes, only fast-sinking particle-attached prokaryotes are taken into account which certainly underestimates the respiration used. All prokaryotic carbon demand (PHPs and PRs) estimates were integrated within RUBALIZ boundaries (i.e. 127m - 751m). Non-sinking prokaryotes PHP rates were integrated using a piecewise model with a single node on the log-data as described in Fuchs et al. (2022). Sinking prokaryotes PHP rates were integrated using power law. Sinking PR were integrated using trapeze because data are only available until 500m and without any *a priori* on the curve shape, this method is certainly the most conservative.

Zooplankton activities are known to be related to POC concentration (Steinberg et al. 2008). Zooplankton respiration data were available only for the cruise D341 when the net POC input into the active mesopelagic layer was 59 mg C m^{-2} d^{-1} (including PIPs) instead of 134 mg C m^{-2} d^{-1} for DY032 (see above). For D341, zooplankton respiration integrated within the active mesopelagic zone (135-726m, Fuchs et al. 2022) was 9 mg C m^{-2} d^{-1}. Zooplankton respiration was integrated using a power law as in Giering et al. (2014). Zooplankton respiration data are missing for DY032, thus we consider this quantity as a percentage of the POC input that we calculate from the D341 data set, i.e. 14.67%. The zooplankton respiration value used here is therefore 17 mg C m^{-2} d^{-1}.

228 *Table 1: Fluxes and their associated values used in this study. Anderson & Tang model's terms*

229 *(Anderson and Tang 2010) corresponding to these fluxes are also shown. Values are integrated*

230 *between 127 and 751m which are boundaries of the active mesopelagic zone defined by* Fuchs

231 *et al. (2022). POC and DOC refer respectively to Particulate and Dissolved Organic Carbon,*

232 *PHP to Prokaryotic Heterotrophic Production, and PR to Prokaryotic Respiration.*

Name	Anderson and Tang's Model term correspondence	Values	units	sources
Net POC input	$D1ex$	117	mg C m^{-2} d^{-1}	Belcher et al. (2016); Boyd et al. (2019)
DOC input	$DOCex$	3	mg C m^{-2} d^{-1}	Giering et al. (2014)
Non-sinking prokaryotes PHP	$F_{BFL} + F_{BAD2}$	1.10E+07	pmol Leu m^{-2} d^{-1}	Baumas et al. (2021)
Sinking prokaryotes PHP	F_{BAD1}	1.02E+06	pmol Leu m^{-2} d^{-1}	Baumas et al. (2021)
Sinking prokaryotes PR	R_{BAD1}	19	mg C m^{-2} d^{-1}	Adapted from Belcher et al. (2016)
Zooplankton respiration	$R_{VA} + R_{VFL} + R_H + R_{Z1:6}$	17	mg C m^{-2} d^{-1}	Adapted from Giering et al. (2014)

233

2.2 Mathematical methods

2.2.1 Parameter estimation

236 The scope of our study is to estimate *in situ* parameters by inverting the model introduced by

237 Anderson and Tang (2010), adapted by Giering et al. (2014). We do not intend to present the

238 model in details here. The details of the equations constituting the version of the model used

239 can be found in the original paper (Anderson and Tang 2010), in the R code available at

240 https://github.com/RobeeF/InverseCarbonBudgetEstim and the specific terms related to

241 variables used are reported in Table 1. The model is calibrated by choosing the set of input

parameters that yields the best fit between the model output and the data. As the model outputs 85 outfluxes, we used a subset of four measurable outfluxes to calibrate the model: the PHP of non-sinking prokaryotes, the PHP of sinking prokaryotes, the PR of sinking prokaryotes and the respiration of zooplankton. These fluxes have been chosen because of their near direct correspondence with outputs of the model linked to the C demand of all groups (sinking prokaryotes, non-sinking prokaryotes, detritivores, bacterivores, and carnivores).

Similarly, the model relies on 20 input parameters (Table S1), which makes the parameter space of significant size and therefore challenging to explore. As such, we first determine the set of parameters that have the largest impact on the output of the model. Then for these parameters, the values that give the best fit between the data and the solution given by the model are determined.

a) Sensitivity of the model to its inputs

In order to reduce the size of the input parameter space, Sobol Indices (Sobol 1993) were used to determine the most influential parameters. These indices enable quantification of the share of the variation of the output that can be imputed to each input parameter.

In essence, the first-order Sobol indices account for the direct influence of an input variable on the output. However, first-order Sobol indices neglect the interactions existing between this input variable and the other input variables. As such, in addition to the first-order Sobol Indices, we used the total Sobol indices introduced by Homma and Saltelli (1996) which encompass both the direct effect of a parameter and also its interactions with the other parameters.

First-order and total Sobol indices were computed to quantify the influence of each parameter over each of the four outfluxes. Only the parameters which had significant Sobol indices (i.e. Sobol indices > 0.20) for at least one outflux were kept.

b) Estimation of the parameters

The parameters which had no substantial effects on the output of the model were set to the values indicated by Anderson and Tang (2010) and Giering et al. (2014) and given in Appendix (Table S1). The other parameters were estimated by minimizing the distance existing between the four outfluxes predicted by the model and their *in situ* measured counterpart. The distance chosen here is a standardized Euclidean distance:

$$\sum_{i=1}^{4}\left(\frac{outflux_{obs,i} - outflux_{model,i}}{outflux_{obs,i}}\right)^2 \qquad (1)$$

where $outflux_{obs,i}$ is the i-th measured flux and $outflux_{model,i}$ its modeled counterpart. The optimization method used is the Nelder-Mead algorithm (Nelder and Mead 1965): if the function to minimize depends on N variables (the number of input parameters here), a simplex constituted by $N + 1$ points is defined. The coordinates of the simplex are updated in turn so that the simplex vertices get closer to the local minimum. Even if this method gives little theoretical guarantees of convergence, it has proven to work well in practice (Lagarias et al. 1998) and has the advantage that it does not require computing the gradient of each outflux with respect to each input parameter.

As the model takes 20 inputs and outputs 85 fluxes, concerns might be raised about the uniqueness of the solution found to minimize the term (1). To make the model identifiable (i.e. sufficiently constrained to estimate the true value of the parameters), the number of input parameters to estimate is limited to the number of output fluxes available, here four. In this respect, the CFs have been fixed to 0.5 kg C mol Leu^{-1} (Estimates without fixing the CFs have however been carried out, see Table S4 in supp. data). This value, contrary to the previously classically used value of 1.55 kg C mol Leu^{-1} (Simon and Azam 1989; Nagata et al. 2010), was determined by Giering and Evans (2022) as the median value of 15 studies conducted in the mesopelagic zone. Doing so, we limit the number of free parameters to be estimated to four so that the model remains identifiable. The model is mostly linear and our experiments have shown the solution to be unique and independent of the initial values taken.

The codes and data to reproduce the results are available at https://github.com/RobeeF/InverseCarbonBudgetEstim

3.Results

3.1 Most sensitive parameters

Using Sobol indices, we identified the most sensitive parameters from the 20 of the Anderson and Tang (2010) model on the 4 fluxes outputs of the model for which we have the measured counterpart (i.e. PHP and PR of sinking prokaryotes, PHP of non-sinking prokaryotes and respiration of zooplankton). All parameter definitions are given in Table S1. For the outflux "PHP of non-sinking prokaryotes", only the $PGE_{non-sinking}$ appears to be sensitive with a Sobol

index of 0.68 meaning that it explains 68% of the variance (Table 2). Fluxes related to sinking prokaryotes, i.e. their PHP and their PR, appear to be highly influenced both by Ψ, α, and $PGE_{sinking}$. For instance, our analysis yields to indices of 0.22 and 0.23 for Ψ, 0.24 and 0.24 for α and 0.27, 0.25 for $PGE_{sinking}$ respectively. Surprisingly, zooplankton respiration is more impacted by the $PGE_{non-sinking}$ (Sobol index of 0.52) than proper zooplankton parameters. All other parameters exhibit Sobol indices below 1%. Total Sobol indices, indicating the part of the variance of fluxes due to the parameter alone and in interaction with the others, were similar to the first-order indices, suggesting no interactions of parameters regarding the variance of fluxes. This sensitivity analysis enabled the identification of Ψ, α, and both PGEs as the most influential parameters, suggesting that their values should be set with particular care. Especially for the $PGE_{non-sinking}$ which can be responsible for more than 50% of the variance of $PHP_{non-sinking}$ and zooplankton respiration. PGEs are growth efficiencies defined as the amount of new prokaryotic biomass produced per unit of organic C substrate assimilated and is a way to relate PHP and PR (del Giorgio and Cole 1998). Ψ corresponds to the percentage of POC consumed by prokaryotes and α to the fraction of hydrolyzed POC which is lost into the surrounding water, i.e. not assimilated by sinking prokaryotes that hydrolyzed it.

Table 2: First-order Sobol indices for the parameters of the model by Anderson and Tang (2010). The definition of each parameter can be found in Table S1. Significant Sobol indices (>0.2) are shown in red. PHP and PR respectively refer to Prokaryotic Heterotrophic Production and to Prokaryotic Respiration.

	ψ	PGE sinking	PGE non-sinking	α	Φv	βv	Kv	Φv	βv	Kv	Φz	βz	λz	Kz	Φh	βh	λh	Kh	ζ	ζ2
Non-sinking prokaryotes PHP	<0.01	0.021	0.681	0.01	<0.01	<0.01	<0.01	0.014	<0.01	0.011	-0.012	<0.01	<0.01	0.015	<0.01	<0.01	<0.01	<0.01	<0.01	<0.01
Sinking prokaryotes PHP	0.222	0.24	<0.01	0.265	<0.01	<0.01	<0.01	<0.01	0.011	<0.01	<0.01	<0.01	<0.01	<0.01	0.011	<0.01	<0.01	-0.012	<0.01	-0.011
Sinking prokaryotes PR	0.225	0.243	<0.01	0.252	-0.019	<0.01	<0.01	<0.01	-0.011	<0.01	<0.01	<0.01	0.012	<0.01	<0.01	<0.01	<0.01	<0.01	<0.01	<0.01
Zooplankton respiration	<0.01	0.023	0.507	<0.01	<0.01	0.014	<0.01	0.064	0.027	0.041	<0.01	<0.01	<0.01	<0.01	<0.01	<0.01	0.028	<0.01	<0.01	<0.01

3.2 Model inversion

The optimization method, described in the material and method section, enabled the determination of the 4 parameters identified as sensitive above: Ψ, α, $PGE_{sinking}$, and $PGE_{non-sinking}$ in the case study of PAP DY032. Table 3 reports the combination found by model inversion. By construction of the procedure (e.g. same number of input and output), the solution is unique, explaining why no confidence intervals are reported. The errors between the four fluxes generated by the model and their measured counterparts were less than 1%, far lower than potential measurement errors. The zooplankton flux was the best matched, followed by the PR of the sinking prokaryotes, the PHP of the non-sinking prokaryotes, and of the sinking prokaryotes.

Table 3: Estimation of the parameters Ψ, α, $PGE_{sinking}$ and $PGE_{non-sinking}$ obtained by inversion of the model by Anderson and Tang (2010). As the model was made identifiable, the solutions are unique, explaining the absence of confidence intervals. The remaining differences between the model outfluxes deriving from the estimated input values and the actual in situ measurements are referred to as "Errors" and are expressed in percentage. PHP, PR, and ZR respectively stand for Prokaryotic Heterotrophic Production, to Prokaryotic Respiration and to Zooplankton Respiration.

Estimations				Errors			
Ψ	α	$PGE_{sinking}$	$PGE_{non-sinking}$	$PHP_{non-sinking}$	$PHP_{sinking}$	$PR_{sinking}$	ZR
0.675	0.777	0.026	0.087	-0.487%	0.524%	0.184%	-0.05%

3.3 C budget

The two PGEs presented above along with CF of 0.5 kg C mol Leu^{-1} were applied to leucine-incorporation rates measurements to build the corresponding active mesopelagic C budget. The resulting C budget was compared with two other C budgets calculated with different sets of parameters. The three active mesopelagic zone C budgets resulting from DY032 measurements or estimation are represented in Fig. 1 with the budget (1) obtained with the classical CF value of 1.55 kg C mol Leu^{-1} and median literature values for PGEs, i.e. 0.07 for $PGE_{non-sinking}$ (Arístegui et al. 2005; Reinthaler et al. 2006; Baltar et al. 2010; Collins et al. 2015) and 0.02 for $PGE_{sinking}$ (Collins et al. 2015); the budget (2) obtained with the parameter values from

Giering et al. (2014) who reconcile C budget, i.e. CF of 0.44 kg C mol Leu^{-1}, PGE$_{non\text{-}sinking}$ of 0.07, and PGE$_{sinking}$ of 0.24 and the budget (3) obtained with a CF, PGE$_{sinking}$ and PGE$_{non\text{-}sinking}$ of 0.5, 0.026 and 0.087, respectively, determined in this study. The combination yielding to the largest discrepancy is the budget (1) (Fig. 1) (discrepancy of -194 mg C m^{-2} d^{-1}). The C input seems to support the zooplankton respiration and total C demand of sinking prokaryotes but not the one of non-sinking prokaryotes especially due to their PR of 218 mg C m^{-2} d^{-1}. Combination of budget (2) and (3) presented both an excess of C (60 and 40 mg C m^{-2} d^{-1} respectively) compared to the biological C demand. These two differ mainly on the PR of sinking prokaryotes which is negligible in combination (2) but which is the second largest flux in the C demand in our study. In all cases, the C demand of non-sinking prokaryotes accounts for most of the total C demand.
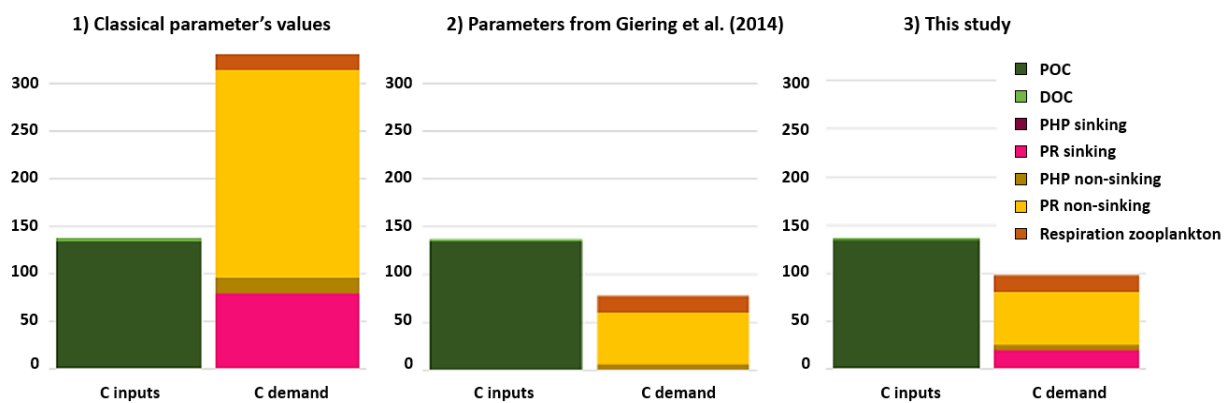
Figure 1: Carbon budget for the active mesopelagic zone estimation resulting from DY032 measurements or estimation and on which different combination of CF (1.55, 0.44 and 0.5 respectively for budget 1) 2) and 3)) , PGE$_{sinking}$ *(0.02, 0.24 and 0.026 respectively for budget 1) 2) and 3)) and* PGE$_{non\text{-}sinking}$ *(0.07, 0.08 and 0.087 respectively for budget 1) 2) and 3)) were applied on leucine incorporation rates of sinking and non-sinking prokaryotes. See Fig. S1 for value details.*

4.Discussion:

As stated in the introduction, the scientific community has struggled to reconcile the mesopelagic carbon budget with measurements and estimates showing a carbon demand often greater than the amount of known organic C sources (e.g. Reinthaler et al. 2006; Steinberg et al. 2008; Burd et al. 2010; Collins et al. 2015; Boyd et al. 2019). Building C budget involves a plethora of parameters whose impacts are overlooked and often neglected, mainly because neither their ideal values nor their underlying mechanism in the water column across space and time are clearly understood. The scientific community is concerned about this issue (e.g. Burd et al. 2010; Giering and Evans 2022), but in the absence of a better option and in an attempt to

encourage comparisons, the same parameter values are universally used. A first step towards this direction was conducted thanks to the RUBALIZ method (Fuchs et al. 2022) which precisely determines the vertical location of the "active mesopelagic zone" and thereby estimates the boundaries between which to integrate C fluxes. In the current study, we pursue this investigation and combine measurements with modeling approaches to investigate the role of sensitive parameters related to the remineralization of POC in the mesopelagic zone.

4.1 Optimization method: Consistency of parameters estimated

The Anderson and Tang (2010) model takes as inputs the measured C inputs as well as 20 parameters related to the activity of organisms such as sinking prokaryotes, non-sinking prokaryotes, zooplankton detritivores, bacterivores, and carnivores. Among the 20 parameters, four have been found to be particularly sensitive in assessing the carbon demands of the various groups: Ψ (percentage of particle consumption by prokaryotes), α (percentage of C hydrolyzed released in surrounding water), $PGE_{non-sinking}$ and $PGE_{sinking}$ (growth efficiencies of sinking and non-sinking prokaryotes). It is interesting to note that zooplankton respiration (which is the sum of detritivores, bacterivores and carnivores respiration) is mostly sensitive to one parameter: $PGE_{non-sinking}$ but not to a parameter specific to zooplankton. This counter-intuitive result suggests a strong synergy between the two model compartments. At this point, it is challenging to establish whether this is the outcome of a complex ecological process or a model artifact.

In the model, the consumption of particles is done by two groups: prokaryotes (Ψ) and detritivores ($1-\Psi$). It can be estimated by taking the average ratio between PHP and ZR. Anderson and Ryabchenko (2009) estimated Ψ using calculations of POC consumption by prokaryotes and zooplanktons between 150 and 1000m performed by Steinberg et al. (2008) in the Pacific. Following this, they set Ψ at 0.76. The inversion of the Anderson and Tang model (2010) leads to a well-identified solution of Ψ, i.e. 0.67 in the case of PAP DY032 cruise. This value is in line with the one used by Anderson and Tang (2010). However, data are lacking to compare and explore variations of Ψ value across seasons, locations or depths. In the model, Ψ participates in the repartition of POC input between prokaryotes and detritivores. Whether for modeling purposes to determine Ψ or to build a C-budget without a model, PHP and ZR are required. It remains too rare to have both together and more future efforts should be devoted to get PHP and ZR concomitantly.

412   Beyond Ψ, according to Sobol indices, **α** is the second parameter of interest. When prokaryotes

413   consume POC using hydrolytic enzymes, a major fraction of the hydrolyzed C is lost to the

414   surrounding environment as DOC (Smith et al. 1992; Vetter et al. 1998). This loss is

415   represented by **α** and is very difficult to quantify accurately. Two major experiments, focused

416   on amino acid hydrolysis, aimed to determine such losses: Smith et al. (1992) and Grossart and

417   Ploug (2001). Smith et al. (1992) sampled particles at 25m and showed that 97% of particulate

418   combined amino acids are released in the surrounding water. Later, Grossart and Ploug (2001)

419   using aggregates from phytoplankton cultures show a loss of POC of 74%. Relying on these

420   two studies, Anderson and Tang (2010) followed by Giering et al. (2014) consider that the

421   value should be lower than that of a fresh detritus and choose a conservative value of 0.5. In

422   the case of these two experiments, only the amino acids are considered and the experiments

423   were conducted under laboratory-controlled settings. However, both, amino acids and sugar

424   are major components of POC, constituting between 40 to 70% of POC in the mesopelagic

425   zone (Wakeham et al. 1997). Conversely, we used unpublished data from PEACETIME cruise

426   (see methods details in supp. data) of *in situ* hydrolysis rates of aminopeptidase and β-

427   glucosydase from sinking prokaryotes (which hydrolyze amino acids and sugar, respectively)

428   that we were able to convert into hydrolyzed carbon fluxes (see measurements and calculation

429   details in supp. data). Unfortunately, total hydrolyzed C fluxes were most of the time below

430   the C demand of the sinking prokaryotes which is unrealistic and probably due to the low

431   amount of POC (sinking POC concentration of <1 mg L^{-1} in the sinking fraction) resulting in

432   insufficient sinking prokaryotes abundance to detect their activity by volume. However, when

433   total hydrolyzed C fluxes were superior to $PHP_{sinking}$ (indicating that some hydrolyzed C is not

434   assimilated and is released), **α** was estimated between 0.19 and 0.79 with a mean of 0.41±0.24

435   and seems to decrease with depth (see calculations details in supp data). This could confirm

436   Grossart and Ploug's (2001) work showing that the older a detritus is, the less enzymatic

437   activity there is and therefore the less amino acid loss. Even if **α** is not measurable easily, this

438   parameter is identified at 0.78 by the inversion method during a post-bloom period at the PAP

439   site. This value is consistent with Smith et al. (1992) and Grossart and Ploug (2001) evidencing

440   high **α** for surface aggregates (0.97) with laboratory-made phytoplankton aggregates (0.74), or

441   with our calculations for the Mediterranean Sea (0.41±0.24), an oligotrophic region. This

442   suggests that the optimization method is a relevant alternative to determine **α**. In addition, **α**

443   corresponds to a release of C in the surrounding water. Regarding the model, the C demand of

444   free-living prokaryotes matches the hydrolyzed C released which constitutes their main C

445   sources. The relationship between enzymatic activities and heterotrophic production of free-

living prokaryotes is well documented in the deep-sea ocean (Cho and Azam 1988; Smith et al. 1992; Hoppe and Ullrich 1999; Tamburini et al. 2002, 2003; Nagata et al. 2010). Total C demand of non-sinking prokaryotes is challenging to measure due to the diversity of existing methods, especially the PR (e.g. Table S2), which leads to an incredibly wide range of estimated values. Subsequently, identifying α via the optimization method could help to avoid these conflicting PR measurements.

The last two sensitive parameters according to Sobol indices were $PGE_{non-sinking}$ and $PGE_{sinking}$. A wide range of $PGE_{non-sinking}$ has been estimated using $PHP_{non-sinking}$ and $PR_{non-sinking}$ in the open ocean (e.g. Sherry et al. 1999; Lemée et al. 2002; Carlson et al. 2004; Arístegui et al. 2005; Reinthaler et al. 2006; Baltar et al. 2009, 2010; Collins et al. 2015). Overall it varies from 0.001 to 0.64 (Collins et al. (2015) and Sherry et al. (1999), respectively). However, these values were produced from different protocols for the PHP (changes in biomass, thymidine or leucine incorporation, each with its own conversion factors and/or constants) and for the PR methods (by ETS measurements, micro-winkler titration, changes in dissolved O_2, or using optodes sensors spots, see Table S2) and correspond to various locations, seasons and depths. These are all valid reasons that can potentially explain the stark contrast in the values reported. If one focuses only on the mesopelagic zone in the North Atlantic, the median is 0.07 (Arístegui et al. 2005; Reinthaler et al. 2006; Baltar et al. 2010; Collins et al. 2015). The optimization method yielded to a value of 0.087 and therefore produces very consistent results for a post-bloom period at the PAP site. Concerning $PGE_{sinking}$, too few values are available. To our knowledge, only Collins et al. (2015) provided *in situ* values associated with sinking prokaryotes (from 0.01 to 0.03) at 150m. This is the only comparison we have, and our value of 0.026 matches this order of magnitude. As a further comparison, the non-integrated data from DY0312 allows us to calculate a $PGE_{sinking}$ (using $PGE_{sinking} = PHP_{sinking}/(PHP_{sinking}+PR_{sinking})$) according to del Giorgio and Cole (1998). The result is thus, a depth-specific PGE instead of a depth-integrated PGE. This led to a variation from 0.033 at 70m to 0.0013 at 500m. Although the lack of datapoints deeper than 500m and the low number of points forces us to stay cautious about these estimates, it may indicate that $PGE_{sinking}$ is not constant throughout the mesopelagic zone and decreases with depth. Constraining conditions due to the increase of hydrostatic pressure and decrease in temperature experienced by prokaryotes attached to sinking particles could explain this decrease in $PGE_{sinking}$ (Stief et al. 2021; Tamburini et al. 2021). Under highly constrained conditions, Russell and Cook (1995) explained that maintaining respiration at the highest possible rate would allow the supply of active membrane transporters which are vital to the cell. This implies a low but optimal PGE (Westerhoff et al. 1983) which could thus

decrease with depth and time as the POC becomes less labile (Grossart and Ploug 2000). On the contrary, the Anderson and Tang (2010) model, and the associated model inversion presented here, is built so that the mesopelagic zone is considered as one homogeneous entity. Explicitly, specifying depth-dependent $PGE_{sinking}$ in the mesopelagic zone could lead to more realistic modeling, but would entail a non-negligible additional model complexity.

It is worth noting that the $PGE_{sinking}$ and $PGE_{non-sinking}$ estimated here rely on a leucine-to-carbon Conversion Factor (CF) of 0.5 kg C mol Leu^{-1}. This value comes from the median of 15 values obtained on the free-living prokaryotes of the mesopelagic zone (between 300 to 1000m), which do not sink and are adapted to their place in the water column (Giering and Evans 2022). However, to our knowledge, there are no such values measured for the specific case of sinking prokaryotes. The latter are surface prokaryotes that have attached to the particles and will experience changes in conditions (e.g. pressure, temperature) linked to their sink (Baumas et al. 2021; Tamburini et al. 2021). The CF depends, among other things, on the leucine fraction in the proteins and the cellular carbon/protein ratio (Kirchman and Ducklow 1993). It is known that stresses can affect the incorporation of leucine into proteins and general protein production (e.g. Young 1968; Welch et al. 1993) and that these parameters can vary with prokaryotic diversity, especially between bacteria and archaea (Bogatyreva et al. 2006). Stresses occur during the descent throughout the water column and sinking prokaryotes experienced a drastic decrease in diversity following the sink at PAP DY032 (Baumas et al. 2021; Tamburini et al. 2021). We can therefore easily imagine that the CF for sinking prokaryotes could be impacted. Despite this, without having further data, we applied the same CF on sinking as the 0.5 recommended by Giering and Evans (2022) for non-sinking prokaryotes.

4.2 Influence on mesopelagic C Budget

As stated in the introduction, mesopelagic C budgets are constructed by applying a CF and a PGE on leucine incorporation rates data to assess prokaryotic C demand. In Fig. 1, we applied three different combinations of CFs and PGEs to the same data. The combination using conventional CF of 1.55 kg C mol Leu^{-1}, $PGE_{non-sinking}$ of 0.07, and $PGE_{sinking}$ of 0.02 led to an aberrant discrepancy such that more than the entire C pool would be remineralized in the active mesopelagic zone and that there would be no source of C to sustain deeper zone life nor sequestration by the BCP. As stated above, this was a recurrent issue in the field (Reinthaler et al. 2006; Steinberg et al. 2008; Burd et al. 2010; Collins et al. 2015; Boyd et al. 2019) with the exception of Giering et al. (2014) who reconcile the C budget of the mesopelagic zone. Giering

et al. (2014) results were mainly due to the difference in CF applied on their data, i.e. 0.44 kg C mol Leu^{-1}. However, from a model point of view, the main difference between C budgets estimated using Giering et al. (2014) parameters and those determined by our optimization method is due to the 10-fold difference between PGE$_{sinking}$ used. Giering et al. (2014) used 0.24 which is the mean of a 14 days incubation experiment during which PGE varied from 0.45 in the first 3 days to 0.04 at the end for riverine aggregates (Grossart and Ploug 2000). Despite the fact that PGE$_{sinking}$ data are very scarce, riverine values of 0.24 seem highly unlikely and inappropriate to mesopelagic sinking prokaryotes compared to what is known in marine environments (e.g. Collins et al. 2015). Indeed, if we consider that enzymes account for a large proportion of the proteins produced by cells (see above) the PGE$_{sinking}$ must be low due to the high metabolic cost of their production (Grossart and Ploug 2000). Finally, the C budget built from a combination of CFs of 0.5 kg C mol Leu^{-1} and PGEs revealed by our optimization method seems the most reasonable option (from the three budgets built, Fig. 1) with an excess of C input of 40 mg C m^{-2} d^{-1}. In this case, PGEs were determined by the model, which in addition to PHP and PR of sinking and non-sinking prokaryotes and zooplankton respiration, also accounts for the production of zooplankton biomass into calculations. We do not have measurements or estimates for the production of zooplankton biomass but based on the model, this biomass production is 11 mg C m^{-2} d^{-1}. Adding this value to the C demand implies a leftover of 29 mg C m^{-2} d^{-1} that is not used and is exported below the active mesopelagic zone via gravitational sinking POC. This value is in accordance with the POC flux estimated from measures at 751m (thus at the exit of our zone): 17 mg C m^{-2} d^{-1}. Being aware of the biases that may exist in the fluxes used as well as in the construction of the model itself, our optimization method enables the determination of realistic values of parameters and thus constructing robust C budgets. As far as we know, the combination of field measurements (using consistently defined integration depths, such as RUBALIZ (Fuchs et al. 2022) with the use of optimization method on the Anderson & Tang model has led to the most complete and realistic mesopelagic carbon budget.

4.3 Model: reliability and potential biases

The Anderson and Tang model (Anderson and Tang 2010) was originally parametrized with 20 input parameters and 85 output fluxes, and is hence by definition an underdetermined model as the number of outputs is higher than the number of inputs. To make the model identifiable, i.e. obtaining unique solutions for each parameter value, the number of parameters allowed to vary, namely: Ψ, α, PGE$_{non\text{-}sinking}$, and PGE$_{sinking}$, was restricted to the number of measurable

549 outputs (here four, PHP$_{sinking}$, PR$_{sinking}$, PHP$_{non\text{-}sinking}$, and zooplankton respiration).

550 Measurement errors (e.g. measurement device errors, *in situ* variabilities, errors due to

551 integration methods) are typically challenging to characterize. Furthermore, even if these four

552 outfluxes well describe the prokaryotic and zooplankton compartment fluxes, one may wonder

553 about the sensitivity of the results to the fact that a given outflux is not available or estimated

554 with error.

555

556 As a result, we have tested two settings: a model inversion without the zooplankton respiration

557 flux (using only three fluxes) and a second setting where the PGEs were estimated from the

558 leucine incorporation rate using freely varying CFs, i.e. with CFs no more fixed at 0.5 as a

559 value. The results are reported in Table S3 and S4. Not using the zooplankton flux to inverse

560 the model mechanically adds some variability to the estimation results, especially concerning

561 Ψ, α, and PGE$_{non\text{-}sinking}$, in decreasing order of variability (Table S3). The PGE$_{sinking}$ was not

562 affected as its confidence interval length was inferior to 10^{-7}: this underlines the very limited

563 interaction between the zooplankton and sinking prokaryote compartments in the model

564 (contrary to the zooplankton and non-sinking prokaryote compartments). Yet, the difference

565 between the four-flux and three-flux parameter estimations was negligible (<1% variation for

566 each estimate), highlighting the robustness of the estimates to the potential unavailability of

567 the zooplankton respiration. On the contrary, as made visible in Table S4, not fixing the CFs

568 to estimate the PGEs created more variations in the PGE estimations, while the estimations of

569 Ψ and α changed by less than 5% with respect to Table 2 estimations. The PGEs of the attached

570 and free-living parameters get significantly closer to their fixed boundaries (10%), while the

571 CFs rise, especially the CF of the attached particles (=1.87 kg C mol Leu^{-1}). Similarly, if PGEs

572 are no longer bounded, the estimates of PGEs (0.17 for attached prokaryotes and 0.23 for free-

573 living prokaryotes) and CFs (3.93 kg C mol Leu^{-1} for attached prokaryotes and 1.53 kg C mol

574 Leu^{-1} for free-living prokaryotes) become unrealistic. This can be explained by the fact that the

575 PGEs and CFs play similar mathematical roles in the current formulation of the model. Hence,

576 without additional fluxes ensuring full model identifiability, one of these two types of

577 quantities needs to be fixed to estimate the other.

578

579 In addition to these sensitivity analyses, an uncertainty analysis has been run by simulating

580 errors in the measurements of the POC, DOC and the four output fluxes (see Table S5 in supp.

581 data). Simulating errors from -10% to 10% for each flux, the estimation of the four parameters

582 of interest were lowly affected: 1%, 2%, 3% and 1% on average for the Ψ, PGE$_{sinking}$, PGE$_{non\text{-}}$

583 $_{sinking}$ and α, respectively. The PGE$_{non\text{-}sinking}$ was mostly sensitive to measurement errors of POC

flux, DOC flux and $PHP_{non-sinking}$ (generating variations of 6%, 5% and 5%, respectively). Similarly, the $PGE_{sinking}$ was logically mostly sensitive to errors in the $PHP_{sinking}$ and $PR_{sinking}$ (generating variations of 6% for both). For the measurement errors, the generated variations all remained under 3% which is reassuring concerning the stability of the estimation.

Finally, the last potential source of estimation bias results from the assumed stationarity hypothesis of the mesopelagic system. For logistical and technical reasons, measurements and sampling between the upper and lower boundary of the mesopelagic zone are typically performed simultaneously. The stationarity assumption is thus a natural foundation ground upon interpretations and models. However, there is a temporal delay in flux variations between the upper layer and lower measurements (Giering et al. 2017; Stange et al. 2017). This delay depends on the particles sinking speed typically ranging from 2 to 1500 m d^{-1} (Alldredge and Silver 1988; Armstrong et al. 2002; Trull et al. 2008; Turner 2015), their morphotype, density and porosity as well as the timing of their production. Strong meteorological events can also perturbate C fluxes from the water column with an increasing time lag over depth (e.g. Pedrosa-Pàmies et al. 2019). Admittedly, C budgets suffer from lack of time integration into the analysis. Our study regarding PAP site is also concerned as it undergoes a substantial seasonality (Cole et al. 2012; Giering et al. 2017). Although, we do not have enough understanding of vertical time lag to change the model and to avoid such bias yet. Some long-term observatories such as BATS in the Bermuda Atlantic or HOT in Hawaii provide biogeochemical flux time series but monthly sampling focuses mostly on the euphotic zone and does not investigate the mesopelagic zone enough. Sampling at discrete times following the sink of a bloom (e.g. Le Moigne et al. 2016) could be a solution, which would nevertheless entail a significant cruise planning effort.

4.4 Grounds for improvements

Anderson & Tang model allowed us to have a comprehensive vision of the remineralization processes in the mesopelagic zone by including the interactions between various compartments, completing *in situ* measurements with a comprehensive vision of the mechanisms at stake. The described inversion of the Anderson & Tang model provided meaningful estimations of the parameters of interest. However, as most models represent complex phenomena, some processes are not fully and properly captured by the model. Below, we provide a list of processes that may help refining mesopelagic C budget estimations.

4.4.1 Other microorganisms

The role of microbial eukaryotes, viruses, and the input of C by chemolithotrophs (Herndl and Reinthaler 2013; Lara et al. 2017; Kuhlisch et al. 2021; Luo et al. 2022) are not included in the model. For instance, eukaryotes can dominate microbial biomass on bathypelagic particles (Bochdansky et al. 2017), and have the potential to promote the aggregation of particles (Jain et al. 2005; Chang et al. 2014; Hamamoto and Honda 2019; Xie et al. 2022). Viruses could be the main cause of prokaryotic and phytoplanktonic mortality. Thus, DOC fluxes could be attributed to them, in particular with the cell lyses they provoke (Fuhrman 2000 and ref within, Lara et al. 2017; Kuhlisch et al. 2021). In the North Atlantic, 9 to 12% of cells could be infected by viruses which would cause a DOC production of $0.1\ \mathrm{mg\ C\ m^{-3}\ d^{-1}}$ (Wilhem and Suttle 1999). For comparison, PHP results on PAP before integration (with a conversion factor of $0.5\ \mathrm{kg\ C\ mol^{-1}}$ Leu) were mostly below this value. In addition, inorganic C fixation by chemoautotrophy would be of the same order of magnitude as $\mathrm{PHP_{non\text{-}sinking}}$ rates (Herndl et al. 2005; Reinthaler et al. 2010). It would be important to verify what microbial eukaryotes, chemolithotrophs or viruses contributions are, even if the poor understanding of these processes currently prevents properly integrating them into models.

4.4.2 Lifestyles

Sinking prokaryotes are poorly considered as they are not sampled with the Niskin bottles classically used in oceanography (Planquette and Sherrell 2012; Baumas et al. 2021). However, the use of the MSC at PAP DY032 allows us to access fractions of particulate organic carbon that will allow us to evaluate the importance of sinking prokaryotes. We have seen that their C demand is not negligible and represents 18% of total C demand. Anderson & Tang model distinguishes sinking particles from neutrally buoyant particles, each with distinct attached communities. Since sampling with MSC only allows us to separate what is sinking from what is not, we merged free-living prokaryotes with those attached to neutrally buoyant particles without distinction. However, unlike free-living prokaryotes, prokaryotes attached to neutrally buoyant particles have access to POC and must produce enzyme activity with different metabolisms than their free-living counterparts. In contrast, prokaryotes attached to neutrally buoyant particles are also different from prokaryotes attached to sinking particles since they do not undergo changes in temperature and pressure related to the sink. They must therefore surely have intrinsically different PGE and associated remineralization rates. It would therefore be valuable to consider them as a third distinct group in laboratory experiments and sampling. Contrary to the sinking or ascending particles which are naturally split by their

sinking/ascending velocity (e.g. respectively Smith et al. 1989; Cowen et al. 2001; McDonnell et al. 2015), no means allow the selective and exclusive sampling of neutrally buoyant particles. The only valid way is to use the MSC to let the sinking particles fall into the lower compartments and to filter the "non-sinking" part to retain the particulate fraction. However, it is known that filtration affects the activities of prokaryotes and generates biases (Edgcomb et al. 2016). This makes investigations of prokaryotes associated with neutrally buoyant particles particularly challenging and future endeavors should urgently attempt to target them.

4.4.3 OC inputs

Continuing in the same line, the inputs of C that the model takes into account are only the gravitational POC and the DOC. We chose to artificially increase the gravitational POC flux to add sources of neutrally buoyant particles in the form of PIPs (eddy subduction pump, metazoans migrations and large-scale physical pumps). Indeed, Boyd et al. (2019) clearly showed that these PIPs can be of paramount importance (here we have estimated them at 51.6% of the gravitational flux). Yet, explicitly describing them in a dedicated compartment of the model could be an improvement for future research, as these neutrally buoyant particles have an effect on the whole system, including the prokaryotes linked to various types of particles and their predators or on particle fragmentation. Given the existence of the neutrally buoyant particle compartment, it is feasible to adapt the model to account for these C inputs. This is even more relevant as new optical instruments have flourished (e.g. Briggs et al. 2013; Giering et al. 2020; Picheral et al. 2022) and would make it easier to better quantify these neutrally buoyant particle fluxes.

4.4.4 *In situ* pressure effect

Our last major concern deals with the fact that neither Niskin nor MSC avoid disruption introduced through the process of depressurization when samples are collected at depth (Tamburini et al. 2013; Garel et al. 2019). Heterotrophic activities associated to non-sinking prokaryotes are known to decrease with depth but were mostly sampled without taking care of the *in situ* pressure (e.g. Turley and Mackie 1994; Arístegui et al. 2009). From our knowledge, some devices such as the $IODA_{6000}$ (Robert 2012) were specifically designed to measure *in situ* PR of non-sinking prokaryotes. However, enigmatically high PR values (2-3 orders of magnitude higher than PHP) are measured by $IODA_{6000}$, making it difficult to have confidence in these *in situ* measured PR rates. During the PEACETIME cruise, we use a pressure-retaining sampler (methods presented in supp data), allowing for the first time to access both PHP_{non-}

686 $_\text{sinking}$ and $PR_\text{non-sinking}$ rates and to compare it with classical depressurization procedures (Fig.
687 S1). We observed that activity rates of non-sinking prokaryotes kept under pressure were
688 always higher when kept at *in situ* hydrostatic pressure than their decompressed counterparts
689 and, surprisingly, seem to increase with depth rather than decrease typically depicted and found
690 when the samples are decompressed (Fig. S1). From a C-budget point of view, taking *in situ*
691 pressure into account will increase C demand of free-living prokaryotes well adapted to their
692 living depth.

693

694 The effect of pressure acts inversely on sinking prokaryotes, as they are surface prokaryotes
695 (unadapted to high-hydrostatic pressure) that undergo a dynamic pressure increase as the
696 particle sinks (Baumas et al. 2021; Tamburini et al. 2021). Besides, repeated results (Tamburini
697 et al. 2006, 2009, 2021; Riou et al. 2018) have shown that, while performing a sinking
698 simulation experiment the activities of sinking prokaryotes are affected during the sink. For
699 instance, they noticed that the aminopeptidase activity was always lower with increasing
700 pressure over time than at atmospheric pressure on diatom aggregates (Tamburini et al. 2006).
701 Handling high-pressure sampling or experiments requires much more effort and material than
702 usual methods. However, it seems highly worthy when investigating both, sinking and non-
703 sinking prokaryotes activities, in regard to C-budget purposes.

704

5. Conclusion

706 By combining *in situ* data from the DY032 cruise at the PAP site with inversion of the
707 Anderson & Tang model which includes known processes from the biological C pump, we
708 provide robust and ecologically realistic estimates of key parameters and to better characterize
709 the patterns at stake.

710 1) We showed that the most sensitive parameters in the model are the ones related to
711   prokaryotes such as prokaryotic growth efficiencies and C hydrolyzed by sinking
712   prokaryotes released to the surrounding water.

713 2) By inversion of Anderson and Tang's model, we determined consistent values of the
714   parameters listed above.

3) We showed that using these values instead of the classical mean from literature or inadequate theoretical values resulted in a more consistent and realistic C-budget than previously considered.

4) Additional measurements are needed to better understand both prokaryotic growth efficiencies and Leucine-to-Carbon conversion factors in the mesopelagic zone. However, we recommend measuring fewer fluxes for which we are confident associated with inversion model procedures in order to access parameter values challenging to measure in other places, cruises, or seasons.

Fig. 2 summarizes processes involved in mesopelagic C budgets estimations and highlights missing knowledges. We attempt to classify the processes according to their degree of understanding (well known, insufficient data or unknown) and point out that majority of these processes require a better understanding. Among others, it is crucial to quantify the roles of microbial eukaryotes, viruses, and chemoautotrophs in the entire process of C budgets. Suspended particles should have a dedicated well-identified compartment in future studies instead of being neglected and drowned into others. Finally, accounting for *in situ* hydrostatic pressure when studying prokaryotic C demand is key. This is because: 1) it may reduce PCD for sinking prokaryotes unadapted to increasing pressure and 2) it may increase PCD for free-living prokaryotes well-adapted to their living depth.

Figure 2: Sinking particles export carbon (C) down to the mesopelagic zone through gravitational POC fluxes where this latter is attenuated to satisfy C demand of different groups of organisms such as prokaryotes living attached to sinking particles, attached to non-sinking particles, or free-living

prokaryotes. In turn, viruses and chemoautotrophs can increase the amount of usable labile C. Quantifying C demand and role on POC fluxes of these different groups is crucial to truly assess C sequestration in the deeper layer of the water column. However, a multitude of uncertainties remains for each group. The quantities enclosed in green are well known, in blue lack data and in pink are unknown. C demand is the sum of heterotrophic production (PHP) and respiration (PR). The understanding of these two quantities is currently better for the free-living prokaryotes whereas data are still insufficient for sinking prokaryotes and even absent for prokaryotes attached to non-sinking particles. Moreover, to build C budgets, these variables are integrated over a few hundred meters of water column and the relationship between in situ pressure and C demand remains often neglected even if this relationship highly depends on the prokaryote type considered (not constant for sinking prokaryotes unadapted to the increased pressure, constant for free-living prokaryotes well adapted to their living depth and constant for prokaryotes attached to non-sinking particles which can be adapted or not if the particle was sinking before being stopped in its sink).

Code/Data availability

The codes and data to reproduce the results are available at https://github.com/RobeeF/InverseCarbonBudgetEstim

Author contribution

The idea was conceived by CB, CT and JCP. Sampling and experiments onboard PEACETIME cruise were conducted by CT and MG. The data processing of PAP DY032 data was conducted by CB with advices from FLM, and the one from PEACETIME data by CB and MG. RF designed the inversion detection methodology and performed the estimation with advices from LM. CB and RF led the writing with significant contributions from all authors.

Acknowledgement

We thank the crew and officers of the R.R.S. DISCOVERY (NERC) for their help during the PAP DY032 cruise and of the N/O Pourquoi Pas? during the PEACETIME cruise. This study is a contribution to the PEACETIME project (MISTRALS CNRS INSU, doi: 10.17600/17000300) managed by Cécile Guieu (LOV) and Karine Desboeufs (LISA). We warmly thank F. Van Wambeke, S. Guasco and B. Zancker for onboard works (enzymatic

activities, sugar and amino acids concentrations measurements) during PEACETIME cruise. We wish to express our gratitude to F. Van Wambeke, S. Giering, T. Anderson and A. Belcher for stimulating and informative discussions. This manuscript is a contribution of the APERO project funded by the National Research Agency under the grant APERO [grant number ANR ANR-21-CE01-0027] and by the French LEFE-Cyber program.

Competing interests

The authors declare that they have no conflict of interest.

References

Alldredge, A. L., and M. W. Silver. 1988. Characteristics, dynamics and significance of marine snow. Progress in Oceanography **20**: 41–82. doi:10.1016/0079-6611(88)90053-5

Anderson, T. R., and V. A. Ryabchenko. 2009. Carbon cycling in the Mesopelagic Zone of the central Arabian Sea: Results from a simple model. Washington DC American Geophysical Union Geophysical Monograph Series **185**: 281–297. doi:10.1029/2007GM000686

Anderson, T. R., and K. W. Tang. 2010. Carbon cycling and POC turnover in the mesopelagic zone of the ocean: Insights from a simple model. Deep Sea Research Part II: Topical Studies in Oceanography **57**: 1581–1592. doi:10.1016/j.dsr2.2010.02.024

Arístegui, J., C. M. Duarte, J. M. Gasol, and L. Alonso-Sáez. 2005. Active mesopelagic prokaryotes support high respiration in the subtropical northeast Atlantic Ocean. Geophysical Research Letters **32**: 1–4. doi:10.1029/2004GL021863

Arístegui, J., J. M. Gasol, C. M. Duarte, and G. J. Herndld. 2009. Microbial oceanography of the dark ocean's pelagic realm. Limnology and Oceanography **54**: 1501–1529. doi:10.4319/lo.2009.54.5.1501

Armstrong, R. A., C. Lee, J. I. Hedges, S. Honjo, and S. G. Wakeham. 2002. A new, mechanistic model for organic carbon fluxes in the ocean based on the quantitative

793   association of POC with ballast minerals. Deep Sea Research Part II: Topical Studies

794   in Oceanography **49**: 219–236. doi:10.1016/S0967-0645(01)00101-1

795 Baltar, F., J. Arístegui, J. M. Gasol, E. Sintes, and G. J. Herndl. 2009. Evidence of

796   prokaryotic metabolism on suspended particulate organic matter in the dark waters of

797   the subtropical North Atlantic. Limnology and Oceanography **54**: 182–193.

798   doi:10.4319/lo.2009.54.1.0182

799 Baltar, F., J. Arístegui, E. Sintes, J. M. Gasol, T. Reinthaler, and G. J. Herndl. 2010.

800   Significance of non-sinking particulate organic carbon and dark CO_2 fixation to

801   heterotrophic carbon demand in the mesopelagic northeast Atlantic. Geophysical

802   Research Letters **37**: n/a-n/a. doi:10.1029/2010GL043105

803 Baumas, C. M. J., F. A. C. Le Moigne, M. Garel, and others. 2021. Mesopelagic microbial

804   carbon production correlates with diversity across different marine particle fractions.

805   The ISME Journal **15**: 1695–1708. doi:10.1038/s41396-020-00880-z

806 Belcher, A., M. Iversen, S. Giering, V. Riou, S. A. Henson, L. Berline, L. Guilloux, and R.

807   Sanders. 2016. Depth-resolved particle-associated microbial respiration in the

808   northeast Atlantic. Biogeosciences **13**: 4927–4943. doi:10.5194/bg-13-4927-2016

809 Bochdansky, A. B., M. A. Clouse, and G. J. Herndl. 2017. Eukaryotic microbes, principally

810   fungi and labyrinthulomycetes, dominate biomass on bathypelagic marine snow. The

811   ISME Journal **11**: 362–373. doi:10.1038/ismej.2016.113

812 Bogatyreva, N. S., A. V. Finkelstein, and O. V. Galzitskaya. 2006. Trend of amino acid

813   composition of proteins of different taxa. J. Bioinform. Comput. Biol. **04**: 597–608.

814   doi:10.1142/S0219720006002016

815 Boyd, P. W., H. Claustre, M. Levy, D. A. Siegel, and T. Weber. 2019. Multi-faceted particle

816   pumps drive carbon sequestration in the ocean. Nature. doi:10.1038/s41586-019-

817   1098-2

818 Briggs, N. T., W. H. Slade, E. Boss, and M. J. Perry. 2013. Method for estimating mean

819   particle size from high-frequency fluctuations in beam attenuation or scattering

820   measurements. Appl. Opt., AO **52**: 6710–6725. doi:10.1364/AO.52.006710

821   Burd, A. B., D. A. Hansell, D. K. Steinberg, and others. 2010. Assessing the apparent

822   imbalance between geochemical and biochemical indicators of meso- and

823   bathypelagic biological activity: What the @$#! is wrong with present calculations of

824   carbon budgets? Deep-Sea Research Part II: Topical Studies in Oceanography

825   1557–1571. doi:10.1016/j.dsr2.2010.02.022

826   Carlson, C. A., S. J. Giovannoni, D. A. Hansell, S. J. Goldberg, R. Parsons, and K. Vergin.

827   2004. Interactions among dissolved organic carbon, microbial processes, and

828   community structure in the mesopelagic zone of the northwestern Sargasso Sea.

829   Limnol. Oceanogr. **49**: 1073–1083. doi:10.4319/lo.2004.49.4.1073

830   Chang, K. J. L., C. M. Nichols, S. I. Blackburn, G. A. Dunstan, A. Koutoulis, and P. D.

831   Nichols. 2014. Comparison of Thraustochytrids Aurantiochytrium sp., Schizochytrium

832   sp., Thraustochytrium sp., and Ulkenia sp. for Production of Biodiesel, Long-Chain

833   Omega-3 Oils, and Exopolysaccharide. Mar Biotechnol 16.

834   Cho, B. C., and F. Azam. 1988. Major role of bacteria in biogeochemical fluxes in the

835   ocean's interior. Nature **332**: 441–443. doi:10.1038/332441a0

836   Cole, H., S. Henson, A. Martin, and A. Yool. 2012. Mind the gap: The impact of missing data

837   on the calculation of phytoplankton phenology metrics. Journal of Geophysical

838   Research: Oceans **117**. doi:10.1029/2012JC008249

839   Collins, J. R., B. R. Edwards, K. Thamatrakoln, J. E. Ossolinski, G. R. DiTullio, K. D. Bidle,

840   S. C. Doney, and B. A. S. Van Mooy. 2015. The multiple fates of sinking particles in

841   the North Atlantic Ocean. Global Biogeochemical Cycles **29**: 1471–1494.

842   doi:10.1002/2014GB005037

843   Cowen, J. P., M. A. Bertram, S. G. Wakeham, R. E. Thomson, J. William Lavelle, E. T.

844   Baker, and R. A. Feely. 2001. Ascending and descending particle flux from

845   hydrothermal plumes at Endeavour Segment, Juan de Fuca Ridge. Deep Sea

846   Research Part I: Oceanographic Research Papers **48**: 1093–1120.

847   doi:10.1016/S0967-0637(00)00070-4

848   Edgcomb, V. P., C. Taylor, M. G. Pachiadaki, S. Honjo, I. Engstrom, and M. Yakimov. 2016.

849   Comparison of Niskin vs. in situ approaches for analysis of gene expression in deep

850   Mediterranean Sea water samples. Deep Sea Research Part II: Topical Studies in

851   Oceanography **129**: 213–222. doi:10.1016/j.dsr2.2014.10.020

852   Eppley, R. W., and B. J. Peterson. 1979. Particulate organic matter flux and planktonic new

853   production in the deep ocean. Nature **282**: 677–680. doi:10.1038/282677a0

854   Fennel, K., J. P. Mattern, S. C. Doney, L. Bopp, A. M. Moore, B. Wang, and L. Yu. 2022.

855   Ocean biogeochemical modelling. Nat Rev Methods Primers **2**: 1–21.

856   doi:10.1038/s43586-022-00154-2

857   Fuchs, R., C. M. J. Baumas, M. Garel, D. Nerini, F. A. C. Le Moigne, and C. Tamburini.

858   2022. A RUpture-Based detection method for the Active mesopeLagIc Zone

859   (RUBALIZ): A crucial step toward rigorous carbon budget assessments. Limnology

860   and Oceanography: Methods **n/a**. doi:10.1002/lom3.10520

861   Fuhrman, J. 2000. Impact of Viruses on Bacterial Processes, *In* Microbial ecology of the

862   oceans. Wiley.

863   Garel, M., P. Bonin, S. Martini, S. Guasco, M. Roumagnac, N. Bhairy, F. Armougom, and C.

864   Tamburini. 2019. Pressure-Retaining Sampler and High-Pressure Systems to Study

865   Deep-Sea Microbes Under In Situ Conditions. Frontiers in Microbiology **10**: 453.

866   doi:10.3389/FMICB.2019.00453

867   Giering, S. L. C., E. L. Cavan, S. L. Basedow, and others. 2020. Sinking Organic Particles in

868   the Ocean—Flux Estimates From in situ Optical Devices. Frontiers in Marine Science

869   **6**. doi:10.3389/fmars.2019.00834

870   Giering, S. L. C., and C. Evans. 2022. Overestimation of prokaryotic production by leucine

871   incorporation—and how to avoid it. Limnology and Oceanography 1–13.

872   doi:10.1002/lno.12032

873   Giering, S. L. C., R. Sanders, R. S. Lampitt, and others. 2014. Reconciliation of the carbon

874   budget in the ocean's twilight zone. Nature **507**: 480–483. doi:10.1038/nature13123

875 Giering, S. L. C., R. Sanders, A. P. Martin, S. A. Henson, J. S. Riley, C. M. Marsay, and D.

876   G. Johns. 2017. Particle flux in the oceans: Challenging the steady state assumption.

877   Global Biogeochemical Cycles **31**. doi:10.1002/2016GB005424

878 del Giorgio, P. A., and J. J. Cole. 1998. BACTERIAL GROWTH EFFICIENCY IN NATURAL

879   AQUATIC SYSTEMS. Annual Review of Ecology and Systematics **29**: 503–541.

880   doi:10.1146/annurev.ecolsys.29.1.503

881 Grossart, H.-P., and H. Ploug. 2000. Bacterial production and growth efficiencies: Direct

882   measurements on riverine aggregates. Limnology and Oceanography **45**: 436–445.

883   doi:10.4319/lo.2000.45.2.0436

884 Grossart, H.-P., and H. Ploug. 2001. Microbial degradation of organic carbon and nitrogen

885   on diatom aggregates. Limnol. Oceanogr. **46**: 267–277.

886   doi:10.4319/lo.2001.46.2.0267

887 Guieu, C., K. Desboeufs, S. Albani, and others. 2020. BIOGEOCHEMICAL dataset collected

888   during the PEACETIME cruise.doi:https://doi.org/10.17882/75747

889 Hamamoto, Y., and D. Honda. 2019. Nutritional intake of Aplanochytrium (Labyrinthulea,

890   Stramenopiles) from living diatoms revealed by culture experiments suggesting the

891   new prey–predator interactions in the grazing food web of the marine ecosystem A.

892   Ianora [ed.]. PLoS ONE **14**: e0208941. doi:10.1371/journal.pone.0208941

893 Henson, S. A., R. Sanders, E. Madsen, P. J. Morris, F. Le Moigne, and G. D. Quartly. 2011.

894   A reduced estimate of the strength of the ocean's biological carbon pump.

895   Geophysical Research Letters **38**: n/a-n/a. doi:10.1029/2011GL046735

896 Herndl, G. J., T. Reinthaler, E. Teira, H. van Aken, C. Veth, A. Pernthaler, and J. Pernthaler.

897   2005. Contribution of *Archaea* to Total Prokaryotic Production in the Deep Atlantic

898   Ocean. Appl Environ Microbiol **71**: 2303–2309. doi:10.1128/AEM.71.5.2303-

899   2309.2005

900 Herndl, G., and T. Reinthaler. 2013. Microbial control of the dark end of the biological pump.

901   Nature Geoscience **6**: 718–724. doi:10.1038/ngeo1921

902   Homma, T., and A. Saltelli. 1996. Importance measures in global sensitivity analysis of

903   nonlinear models. Reliability Engineering & System Safety **52**: 1–17.

904   doi:10.1016/0951-8320(96)00002-6

905   Hoppe, H., and S. Ullrich. 1999. Profiles of ectoenzymes in the Indian Ocean: phenomena of

906   phosphatase activity in the mesopelagic zone. Aquat. Microb. Ecol. **19**: 139–148.

907   doi:10.3354/ame019139

908   Iversen, M. H., N. Nowald, H. Ploug, G. A. Jackson, and G. Fischer. 2010. High resolution

909   profiles of vertical particulate organic matter export off Cape Blanc, Mauritania:

910   Degradation processes and ballasting effects. Deep Sea Research Part I:

911   Oceanographic Research Papers **57**: 771–784. doi:10.1016/j.dsr.2010.03.007

912   Jain, R., S. Raghukumar, R. Tharanathan, and N. B. Bhosle. 2005. Extracellular

913   Polysaccharide Production by Thraustochytrid Protists. Mar Biotechnol **7**: 184–192.

914   doi:10.1007/s10126-004-4025-x

915   Jannasch, H. W., and C. D. Taylor. 1984. Deep-Sea Microbiology. Annual Review of

916   Microbiology **38**: 487–487. doi:10.1146/annurev.mi.38.100184.002415

917   Kiørboe, T. 2003. Marine snow microbial communities: scaling of abundances with

918   aggregate size. Aquatic Microbial Ecology **33**: 67–75. doi:10.3354/ame033067

919   Kiorboe, T., H.-P. Grossart, H. Ploug, and K. Tang. 2002. Mechanisms and Rates of

920   Bacterial Colonization of Sinking Aggregates. Applied and Environmental

921   Microbiology **68**: 3996–4006. doi:10.1128/AEM.68.8.3996-4006.2002

922   Kiorboe, T., K. Tang, H.-P. Grossart, and H. Ploug. 2003. Dynamics of Microbial

923   Communities on Marine Snow Aggregates: Colonization, Growth, Detachment, and

924   Grazing Mortality of Attached Bacteria. Applied and Environmental Microbiology **69**:

925   3036–3047. doi:10.1128/AEM.69.6.3036-3047.2003

926   Kirchman, D., E. K'nees, and R. Hodson. 1985. Leucine incorporation and its potential as a

927   measure of protein synthesis by bacteria in natural aquatic systems. Applied and

928   Environmental Microbiology **49**: 599–607. doi:10.1128/aem.49.3.599-607.1985

929 Kirchman, D. L., and H. W. Ducklow. 1993. Estimating Conversion Factors for the Thymidine

930   and Leucine Methods for Measuring Bacterial Production, *In* Handbook of Methods in

931   Aquatic Microbial Ecology. Lewis publishers.

932 Koski, M., B. Valencia, R. Newstead, and C. Thiele. 2020. The missing piece of the upper

933   mesopelagic carbon budget? Biomass, vertical distribution and feeding of aggregate-

934   associated copepods at the PAP site. Progress in Oceanography **181**: 102243.

935   doi:10.1016/j.pocean.2019.102243

936 Kuhlisch, C., G. Schleyer, N. Shahaf, F. Vincent, D. Schatz, and A. Vardi. 2021. Viral

937   infection of algal blooms leaves a unique metabolic footprint on the dissolved organic

938   matter in the ocean. Science Advances **7**: eabf4680. doi:10.1126/sciadv.abf4680

939 Kwon, E. Y., F. Primeau, and J. L. Sarmiento. 2009. The impact of remineralization depth on

940   the air–sea carbon balance. Nature Geosci **2**: 630–635. doi:10.1038/ngeo612

941 Lagarias, J. C., J. A. Reeds, M. H. Wright, and P. E. Wright. 1998. Convergence properties

942   of the Nelder-Mead simplex method in low dimensions. SIAM Journal on

943   Optimization **9**: 112–147. doi:10.1137/S1052623496303470

944 Lampitt, R. S., B. Boorman, L. Brown, and others. 2008. Particle export from the euphotic

945   zone: Estimates using a novel drifting sediment trap, 234Th and new production.

946   Deep Sea Research Part I: Oceanographic Research Papers **55**: 1484–1502.

947   doi:10.1016/j.dsr.2008.07.002

948 Lara, E., D. Vaqué, E. L. Sà, and others. 2017. Unveiling the role and life strategies of

949   viruses from the surface to the dark ocean. Sci. Adv. **3**: e1602565.

950   doi:10.1126/sciadv.1602565

951 Le Moigne, F. A. C. 2019. Pathways of organic carbon downward transport by the oceanic

952   biological carbon pump. Frontiers in Marine Sciences **6**: 1–8.

953   doi:10.3389/fmars.2019.00634

954 Le Moigne, F. A. C., S. A. Henson, E. Cavan, and others. 2016. What causes the inverse

955   relationship between primary production and export efficiency in the Southern

956   Ocean? Geophysical Research Letters **43**: 4457–4466. doi:10.1002/2016GL068480

957   Lemée, R., E. Rochelle-Newall, F. Van Wambeke, M. Pizay, P. Rinaldi, and J. Gattuso.

958   2002. Seasonal variation of bacterial production, respiration and growth efficiency in

959   the open NW Mediterranean Sea. Aquatic Microbial Ecology **29**: 227–237.

960   doi:10.3354/ame029227

961   Luo, E., A. O. Leu, J. M. Eppley, D. M. Karl, and E. F. DeLong. 2022. Diversity and origins of

962   bacterial and archaeal viruses on sinking particles reaching the abyssal ocean. The

963   ISME Journal 1–9. doi:10.1038/s41396-022-01202-1

964   Marsay, C. M., R. J. Sanders, S. A. Henson, K. Pabortsava, E. P. Achterberg, and R. S.

965   Lampitt. 2015. Attenuation of sinking particulate organic carbon flux through the

966   mesopelagic ocean. Proceedings of the National Academy of Sciences **112**: 1089–

967   1094. doi:10.1073/pnas.1415311112

968   Martin, J. H., G. A. Knauer, D. M. Karl, and W. W. Broenkow. 1987. VERTEX: carbon cycling

969   in the northeast Pacific. Deep Sea Research Part A. Oceanographic Research

970   Papers **34**: 267–285. doi:10.1016/0198-0149(87)90086-0

971   McDonnell, A. M. P., P. J. Lam, C. H. Lamborg, and others. 2015. The oceanographic

972   toolbox for the collection of sinking and suspended marine particles. Progress in

973   Oceanography **133**: 17–31. doi:10.1016/j.pocean.2015.01.007

974   Nagata, T., C. Tamburini, J. Arístegui, and others. 2010. Emerging concepts on microbial

975   processes in the bathypelagic ocean – ecology, biogeochemistry, and genomics.

976   Deep Sea Research Part II: Topical Studies in Oceanography **57**: 1519–1536.

977   doi:10.1016/j.dsr2.2010.02.019

978   Nelder, J. A., and R. Mead. 1965. A Simplex Method for Function Minimization. The

979   Computer Journal **7**: 308–313. doi:10.1093/comjnl/7.4.308

980   Pedrosa-Pàmies, R., M. H. Conte, J. C. Weber, and R. Johnson. 2019. Hurricanes Enhance

981   Labile Carbon Export to the Deep Ocean. Geophysical Research Letters **46**: 10484–

982   10494. doi:10.1029/2019GL083719

983   Picheral, M., C. Catalano, D. Brousseau, and others. 2022. THE UNDERWATER VISION

984   PROFILER 6: AN IMAGING SENSOR OF PARTICLE SIZE SPECTRA AND PLANKTON, FOR

985 AUTONOMOUS AND CABLED PLATFORMS. Limnology & Ocean Methods **20**: 115–129.

986 doi:10.1002/lom3.10475

987 Planquette, H., and R. M. Sherrell. 2012. Sampling for particulate trace element

988 determination using water sampling bottles: methodology and comparison to in situ

989 pumps. Limnology and Oceanography: Methods **10**: 367–388.

990 doi:10.4319/lom.2012.10.367

991 Reinthaler, T., H. M. van Aken, and G. J. Herndl. 2010. Major contribution of autotrophy to

992 microbial carbon cycling in the deep North Atlantic's interior. Deep Sea Research

993 Part II: Topical Studies in Oceanography **57**: 1572–1580.

994 doi:10.1016/j.dsr2.2010.02.023

995 Reinthaler, T., H. van Aken, C. Veth, J. Arístegui, C. Robinson, P. J. L. B. Williams, P.

996 Lebaron, and G. J. Herndl. 2006. Prokaryotic respiration and production in the meso-

997 and bathypelagic realm of the eastern and western North Atlantic basin. Limnology

998 and Oceanography **51**: 1262–1273. doi:10.4319/lo.2006.51.3.1262

999 Riley, J. S., R. Sanders, C. Marsay, F. A. C. Le Moigne, E. P. Achterberg, and A. J. Poulton.

1000 2012. The relative contribution of fast and slow sinking particles to ocean carbon

1001 export. Global Biogeochemical Cycles **26**: 1–10. doi:10.1029/2011GB004085

1002 Riou, V., J. Para, M. Garel, and others. 2018. Biodegradation of Emiliania huxleyi

1003 aggregates by a natural Mediterranean prokaryotic community under increasing

1004 hydrostatic pressure. Progress in Oceanography **163**: 271–281.

1005 doi:10.1016/j.pocean.2017.01.005

1006 Robert, A. 2012. Minéralisation in situ de la matière organique le long de la colonne d'eau :

1007 application sur une station eulérienne. These de doctorat. Aix-Marseille.

1008 Russell, J. B., and G. M. Cook. 1995. Energetics of Bacterial Growth: Balance of Anabolic

1009 and Catabolic Reactions. MICROBIOL. REV. **59**: 15.

1010 Saint-Béat, B., B. D. Fath, C. Aubry, and others. 2020. Contrasting pelagic ecosystem

1011 functioning in eastern and western Baffin Bay revealed by trophic network modeling.

1012 Elementa: Science of the Anthropocene **8**. doi:10.1525/elementa.397

1013   Saint-Béat, B., F. Maps, and M. Babin. 2018. Unraveling the intricate dynamics of planktonic

1014   Arctic marine food webs. A sensitivity analysis of a well-documented food web

1015   model. Progress in Oceanography **160**: 167–185. doi:10.1016/j.pocean.2018.01.003

1016   Sherry, N. D., P. W. Boyd, K. Sugimoto, and P. J. Harrison. 1999. Seasonal and spatial

1017   patterns of heterotrophic bacterial production, respiration, and biomass in the

1018   subarctic NE Pacific. Deep Sea Research Part II: Topical Studies in Oceanography

1019   **46**: 2557–2578. doi:10.1016/S0967-0645(99)00076-4

1020   Siegel, D. A., K. O. Buesseler, M. J. Behrenfeld, and others. 2016. Prediction of the Export

1021   and Fate of Global Ocean Net Primary Production: The EXPORTS Science Plan.

1022   Frontiers in Marine Science **3**: 22. doi:10.3389/fmars.2016.00022

1023   Simon, M., and F. Azam. 1989. Protein content and protein synthesis rates of planktonic

1024   marine bacteria. Marine Ecology Progress Series. doi:10.3354/meps051201

1025   Smith, D. C., M. Simon, A. L. Alldredge, and F. Azam. 1992. Intense hydrolytic enzyme

1026   activity on marine aggregates and implications for rapid particle dissolution. Nature

1027   **359**: 139–142. doi:10.1038/359139a0

1028   Smith, K. L., P. M. Williams, and E. R. M. Druffel. 1989. Upward fluxes of particulate organic

1029   matter in the deep North Pacific. Nature **337**: 724–726. doi:10.1038/337724a0

1030   Sobol, M. 1993. Sensitivity Estimates for Nonlinear Mathematical Models. 8.

1031   Stange, P., L. T. Bach, F. a. C. Le Moigne, J. Taucher, T. Boxhammer, and U. Riebesell.

1032   2017. Quantifying the time lag between organic matter production and export in the

1033   surface ocean: Implications for estimates of export efficiency. Geophysical Research

1034   Letters **44**: 268–276. doi:10.1002/2016GL070875

1035   Steinberg, D. K., B. A. S. Van Mooy, K. O. Buesseler, P. W. Boyd, T. Kobari, and D. M. Karl.

1036   2008. Bacterial vs. zooplankton control of sinking particle flux in the ocean's twilight

1037   zone. Limnology and Oceanography **53**: 1327–1338. doi:10.4319/lo.2008.53.4.1327

1038   Stief, P., M. Elvert, and R. N. Glud. 2021. Respiration by "marine snow" at high hydrostatic

1039   pressure: Insights from continuous oxygen measurements in a rotating pressure

1040   tank. Limnol Oceanogr **66**: 2797–2809. doi:10.1002/lno.11791

1041 Tamburini, C., M. Boutrif, M. Garel, R. R. Colwell, and J. D. Deming. 2013. Prokaryotic

1042   responses to hydrostatic pressure in the ocean–a review. Environmental

1043   microbiology reports **15**: 1262–1274.

1044 Tamburini, C., J. Garcin, and A. Bianchi. 2003. Role of deep-sea bacteria in organic matter

1045   mineralization and adaptation to hydrostatic pressure conditions in the NW

1046   Mediterranean Sea. Aquatic Microbial Ecology **32**: 209–218. doi:10.3354/ame032209

1047 Tamburini, C., J. Garcin, G. Grégori, K. Leblanc, P. Rimmelin, and D. L. Kirchman. 2006.

1048   Pressure effects on surface Mediterranean prokaryotes and biogenic silica

1049   dissolution during a diatom sinking experiment. Aquatic Microbial Ecology **43**: 267–

1050   276. doi:10.3354/ame043267

1051 Tamburini, C., J. Garcin, M. Ragot, and A. Bianchi. 2002. Biopolymer hydrolysis and

1052   bacterial production under ambient hydrostatic pressure through a 2000m water

1053   column in the NW Mediterranean. Deep Sea Research Part II: Topical Studies in

1054   Oceanography **49**: 2109–2123. doi:10.1016/S0967-0645(02)00030-9

1055 Tamburini, C., M. Garel, A. Barani, and others. 2021. Increasing Hydrostatic Pressure

1056   Impacts the Prokaryotic Diversity during Emiliania huxleyi Aggregates Degradation.

1057   Water **13**: 2616. doi:10.3390/w13192616

1058 Tamburini, C., M. Goutx, C. Guigue, and others. 2009. Effects of hydrostatic pressure on

1059   microbial alteration of sinking fecal pellets. Deep Sea Research Part II: Topical

1060   Studies in Oceanography **56**: 1533–1546. doi:10.1016/j.dsr2.2008.12.035

1061 Tarantola, A. 2005. Inverse Problem Theory and Methods for Model Parameter Estimation,

1062   Society for Industrial and Applied Mathematics.

1063 Tian, R. C., A. F. Ve, B. Klein, T. Packard, S. Roy, C. Savenko, and N. Silverberg. 2000.

1064   E!ects of pelagic food-web interactions and nutrient remineralization on the

1065   biogeochemical cycling of carbon: a modeling approach. 26.

1066 Trull, T. W., S. G. Bray, K. O. Buesseler, C. H. Lamborg, S. Manganini, C. Moy, and J.

1067   Valdes. 2008. In situ measurement of mesopelagic particle sinking rates and the

1068   control of carbon transfer to the ocean interior during the Vertical Flux in the Global

1069   Ocean (VERTIGO) voyages in the North Pacific. Deep Sea Research Part II: Topical

1070   Studies in Oceanography **55**: 1684–1695. doi:10.1016/j.dsr2.2008.04.021

1071   Turley, C., and P. Mackie. 1994. Biogeochemical significance of attached and free-living

1072   bacteria and the flux of particles in the NE Atlantic Ocean. Marine Ecology Progress

1073   Series **115**: 191–203. doi:10.3354/meps115191

1074   Turner, J. T. 2015. Zooplankton fecal pellets, marine snow, phytodetritus and the ocean's

1075   biological pump. Progress in Oceanography **130**: 205–248.

1076   doi:10.1016/j.pocean.2014.08.005

1077   Vetter, Y. A., J. W. Deming, P. A. Jumars, and B. B. Krieger-Brockett. 1998. A Predictive

1078   Model of Bacterial Foraging by Means of Freely Released Extracellular Enzymes.

1079   Microb Ecol **36**: 75–92. doi:10.1007/s002489900095

1080   Wakeham, S. G., C. Lee, J. I. Hedges, P. J. Hernes, and M. J. Peterson. 1997. Molecular

1081   indicators of diagenetic status in marine organic matter. Geochimica et

1082   Cosmochimica Acta **61**: 5363–5369. doi:10.1016/S0016-7037(97)00312-8

1083   Weiss, M. S., U. Abele, J. Weckesser, W. Welte, E. Schiltz, and G. E. Schulz. 1991.

1084   Molecular architecture and electrostatic properties of a bacterial porin. Science **254**:

1085   1627–1630. doi:10.1126/science.1721242

1086   Welch, W. J., M. -j. Gething, A. R. Clarke, and others. 1993. Heat shock proteins functioning

1087   as molecular chaperones: their roles in normal and stressed cells. Philosophical

1088   Transactions of the Royal Society of London. Series B: Biological Sciences **339**:

1089   327–333. doi:10.1098/rstb.1993.0031

1090   Westerhoff, H. V., K. J. Hellingwerf, and K. Van Dam. 1983. Thermodynamic efficiency of

1091   microbial growth is low but optimal for maximal growth rate. Proc. Natl. Acad. Sci.

1092   U.S.A. **80**: 305–309. doi:10.1073/pnas.80.1.305

1093   Wilhem, W., and C. A. Suttle. 1999. Viruses and Nutrient Cycles in the Sea. **49**: 8.

1094   Xie, N., M. Bai, L. Liu, and others. 2022. Patchy Blooms and Multifarious Ecotypes of

1095   Labyrinthulomycetes Protists and Their Implication in Vertical Carbon Export in the

1096   Pelagic Eastern Indian Ocean A.L. Dos Santos [ed.]. Microbiol Spectr **10**: e00144-22.

1097   doi:10.1128/spectrum.00144-22

1098   Young, H. L. 1968. Uptake and Incorporation of Exogenous Leucine in Bacterial Cells under

1099   High Oxygen Tension. Nature **219**: 1068–1069. doi:10.1038/2191068a0

1100